

Myocardial Remodeling after Large Infarcts in Rat Converts Post Rest-Potential in Force Decay

Danilo Sales Bocalini¹, Leonardo dos-Santos⁴, Ednei Luiz Antonio¹, Alexandra Alberta dos Santos¹, Ana Paula Dave³, Luciana Venturini Rossoni², Dalton Valentim Vassallo⁵, Paulo José Ferreira Tucci¹

Departamento de Medicina - Divisão de Cardiologia - Universidade Federal de São Paulo¹; Departamento de Fisiologia e Biofísica - Instituto de Ciências Biomédicas - Universidade de São Paulo², São Paulo, SP; Departamento de Biologia Estrutural e Funcional - Instituto de Biologia - Universidade Estadual de Campinas³, Campinas, SP; Departamento de Ciências Fisiológicas - Universidade Federal do Espírito Santo⁴; Departamento de Ciências Morfofuncionais - Escola Superior de Ciências da Santa Casa de Misericórdia⁵, Vitória, ES, Brazil

Abstract

Background: Post-rest contraction (PRC) of cardiac muscle provides indirect information about the intracellular calcium handling.

Objective: Our aim was to study the behavior of PRC, and its underlying mechanisms, in rats with myocardial infarction.

Methods: Six weeks after coronary occlusion, the contractility of papillary muscles (PM) obtained from sham-operated (C, n=17), moderate infarcted (MMI, n=10) and large infarcted (LMI, n=14) rats was evaluated, following rest intervals of 10 to 60 seconds before and after incubation with lithium chloride (Li⁺) substituting sodium chloride or ryanodine (Ry). Protein expression of SR Ca(2+)-ATPase (SERCA2), Na⁺/Ca²⁺ exchanger (NCX), phospholamban (PLB) and phospho-Ser(16)-PLB were analyzed by Western blotting.

Results: MMI exhibited reduced PRC potentiation when compared to C. Opposing the normal potentiation for C, post-rest decays of force were observed in LMI muscles. In addition, Ry blocked PRC decay or potentiation observed in LMI and C; Li⁺ inhibited NCX and converted PRC decay to potentiation in LMI. Although MMI and LMI presented decreased SERCA2 (72±7% and 47±9% of Control, respectively) and phospho-Ser¹⁶-PLB (75±5% and 46±11%, respectively) protein expression, overexpression of NCX (175±20%) was only observed in LMI muscles.

Conclusion: Our results showed, for the first time ever, that myocardial remodeling after MI in rats may change the regular potentiation to post-rest decay by affecting myocyte Ca(2+) handling proteins. (Arq Bras Cardiol 2012;98(3):243-251)

Keywords: Ventricular remodeling; myocardial infarction; muscle relaxation; muscle strength; Rats.

Introduction

In the cardiac muscle, both transsarcolemmal calcium (Ca²⁺) influx and sarcoplasmic reticulum (SR) Ca²⁺ release contribute to the myofilament activation during contraction and in the majority of mammals, the Ca²⁺-induced Ca²⁺ release from SR is quantitatively dominant¹⁻³. The basic cellular mechanisms of cardiac muscle contraction are significantly modulated by the rhythm of stimulation. Thus, changes in rate and rhythm are frequently used as experimental maneuvers to evaluate the behavior or disclose abnormalities of Ca²⁺ kinetics on the excitation-contraction coupling³. Accordingly, post-rest contraction (PRC) allows indirect evaluation of the SR function^{2,4,5}. In the myocardium of normal rats, PRC is potentiated due to the additional Ca²⁺ accumulated in the SR during the pause due to SR Ca²⁺-ATPase (SERCA2) activity and the increased fractional Ca²⁺ release^{2,5} upon activation. On the other hand, PRC is negatively modulated by the Ca²⁺ efflux throughout the Na⁺/Ca²⁺ exchanger (NCX)^{1,2,6,7}.

The ventricular remodelling that follows myocardial infarction (MI) often leads to impaired contractile function of the spared myocardium^{8,11} and is associated with defective intracellular Ca²⁺ handling^{12,13}. As a result, it has been proposed that post-rest potentiation may be altered pathologically by an alteration in calcium kinetics^{14,15}. Previous reports described reduction of the post-rest potentiation in left ventricular papillary muscles from rats with healed MI of different infarct sizes^{9,10}. Recently, we identified, for the first time, decay of the post-rest contractions in rats with chronic heart failure¹⁶. Since the pathophysiological mechanisms underlying the genesis of post-rest contraction in the rat myocardium after remodeling are not completely defined, in this report, we investigated the PRC of left ventricular papillary muscle derived from the MI, and its relationship with the molecular remodeling of the primary Ca²⁺-handling proteins.

Methods

Animals

Wistar rats weighing 180 to 220 g were handled and used according to the *Principles of Laboratory Animal Care* (NIH publication No. 86-23, revised 1985) and the protocol was approved by the local *Research and Ethics Committee of the Universidade Federal de São Paulo* (CEP#0340/08).

Mailing Address: Danilo Sales Bocalini •

Rua General Chagas Santos, 392 - Saúde - 04146-050 - São Paulo, SP, Brasil
E-mail: bocalini@fcr.epm.br

Manuscript received 31 May, 2011, revised manuscript received September 13, 2011; accepted September 20, 2011.

Experimental myocardial infarction

The MI was produced by permanent coronary artery ligation as described by our laboratory in previous publications^{11,17}. Under anesthesia (ketamine 50 mg/kg and xylazine 10 mg/kg, intraperitoneally) and artificial ventilation (Harvard Rodent Ventilator, model 863; Harvard Apparatus, Holliston, MA), a left thoracotomy was briefly performed. The heart was exteriorized and the left anterior descending coronary artery ligated with 6-0 polypropylene suture. The heart was quickly repositioned and the thorax was closed. Sham-operated rats were considered the control group (C). All morphological and functional outcomes were assessed six weeks after MI production.

Global cardiac function and morphology

In order to characterize the MI and heart dimensions and function, Doppler echocardiography was performed in anesthetized animals (same mixture of ketamine plus xylazine) six weeks after surgery. These procedures were performed by one observer blind to the animal condition, using an HP SONOS 5500 instrument (Philips Medical System, Andover, MA, USA) with a 12-MHz transducer at a depth of 2 cm, according to previously described methodology^{11,17,18}. Transverse images were obtained at basal (at the tip of the mitral valve leaflets), middle (at the papillary muscle level) and apical (distal to the papillary muscle but beyond the cavity cap) levels. Infarct size was estimated as the subjective identification of akinesis or dyskinesis of the left ventricle (LV) wall on each transverse plane and presented as the length of the arc corresponding to the segment of the MI scar in relation to the total perimeter of the endocardial border of LV. We recently demonstrated that this echocardiographic measurement presents satisfactory agreement with histochemical staining¹⁸. Infarcted animals were divided into two groups, according to the MI size: one group composed of rats with moderate MI, between 20 and 39% of LV (MMI), and another group of rats with MI larger than 39% of LV (LMI).

The end-diastolic and end-systolic LV diameters were measured from the transverse parasternal view using M-mode images. Systolic function was defined by fractional shortening, and calculated as the average of percent change between the diastolic and systolic diameters. Diastolic function was analyzed by the mitral diastolic influx velocity curve on the pulsed-wave Doppler. From the 4-chamber view, peak E-wave and A-wave velocities were acquired and E/A ratio was calculated.

Isolated cardiac muscle mechanics

Immediately after the echocardiographic examination, *in vitro* preparations of isolated papillary muscle from the LV were performed¹⁹. The heart was quickly removed and placed in oxygenated Krebs-Henseleit buffered solution at 29°C. The posterior papillary muscle of the LV was carefully dissected and vertically mounted in an organ bath heated to 29°C and 100% oxygenated. The muscle was attached to an isometric force transducer (GRASS FT-03, Astro-Med, Inc. RI, USA) connected to a micrometer for adjustments of muscle length. The composition of the Krebs-Henseleit solution was as follows (in mM): 135 NaCl; 4.69 KCl; 1.5 CaCl₂; 1.16 MgSO₄; 1.18 KH₂PO₄; 5.50 glucose; 10 U insulin and 20 HEPES, buffered at pH 7.4. Preparations were stimulated at 0.2 Hz, using 5 ms square-wave pulses through

parallel platinum electrodes at voltages adjusted to approximately 10% greater than the minimum required to produce maximal mechanical response. After 60 min of stabilization at low loading condition, the muscle was loaded to contract isometrically and stretched to peak length of its length-tension curve (L_{max}). Tests were performed at L_{max} (optimal length for contraction), and isometric tension was evaluated by force normalized to the muscle cross-sectional area ($g\ mm^{-2}$). The following parameters were obtained: resting tension (RT), peak of developed tension (DT) and its first derivative (dT/dt), time to peak tension (TPT), and time to 50% of relaxation (TR50). Relative PRCs were measured in the three experimental groups using pause durations of 10, 15, 30, 45 and 60 sec. Relative PRC was expressed as the amplitude of post-rest DT divided by the steady-state DT. To investigate the role of the SR and the NCX on the PRC, this protocol was repeated in the presence of 1 μ M ryanodine to inhibit SR function²⁰, and using a modified KH solution with zero [Na⁺] and 135 mM of lithium chloride (Li⁺) to inhibit NCX function²¹. Li⁺ was substituted for Na⁺ because it passes through the Na⁺ channel, maintaining myocyte excitability while the membrane exchangers are not able to use Li⁺ for exchange²¹.

Biometrical parameters

After papillary muscle was removed, left and right ventricles were separated and weighed. The right lung was also excised and weighed. After drying at 70°C for 12 h, the pulmonary water content (PWC), considering a congestion index, was determined using the following equation: PWC (%) = (weight loss after drying / wet weight) \times 100.

Protein expression of SERCA2, phospholamban and NCX

Protein content was analyzed in samples of LV of LMI, MMI and C groups after excision of the papillary muscles and infarct scar. Tissue homogenates were analyzed by Western blotting according to previously described protocols⁵ to compare the protein expression of SERCA2, phospholamban (PLB), phospho-Ser¹⁶-PLB and NCX in all experimental groups. Samples of non-infarcted myocardium were rapidly frozen at -70°C. Tissues were homogenized in ice-cold extraction buffer (Tris 50 mM, EDTA 1 mM and saccharose 250 mM, pH 7.4) using Polytron (Polytron® PT2100, Kinematica AG, Littau, LU, SWI). To prepare the microsomal fractions of proteins, an initial centrifugation was made at 10,000 \times g for 10 min at 4°C. The supernatant was centrifuged at 100,000 \times g for 60 min. The pellet, representing the microsomal fraction, was resuspended in Tris-EDTA buffer (Tris 50 mM, EDTA 1.0 mM, pH 7.4). Twenty-five micrograms of protein from the LV and pre-stained molecular SDS-PAGE standards (Bio-Rad, Laboratories, Hercules, CA, USA) were electrophoretically separated on a 7.5% or 12% SDS-PAGE (for NCX or SERCA2 and PLB, respectively) and then transferred to polyvinylidene difluoride membranes overnight at 4°C, using a Mini Trans-Blot Transfer Cell system (Bio-Rad) containing Tris 25 mM, glycine 190mM, methanol 20% and SDS 0.05%. Transferring efficiency and protein charging equality were verified by gel Ponceau S 1% staining (Caledon laboratories, Georgetown, ON, CAN), previously validated as an efficient alternative to sample quality and loading control²². Then the membrane was blocked for 60 min at room temperature in Tris-buffered solution (Tris 10 mM, NaCl 100 mM, Tween-20 0.1%, pH 7.4) with 5% powdered

non-fat milk. Next, the membrane was incubated overnight at 4°C with anti-NCX1 rat monoclonal antibodies (1:1500 dilution, Swant® Swiss antibodies, Bellinzona, CH, SWI), anti-SERCA2 rat monoclonal antibodies (1:2500 dilution, Abcam Inc., MA, USA), anti-PLB rat monoclonal antibodies (0.25 µg/ml, Upstate Biotechnology, Lake Placid, NY, USA) or anti-phospho-Ser¹⁶-PLB rat monoclonal antibodies (1:1000, Upstate Biotechnology, Lake Placid, NY, USA). After washing, the membrane was incubated for 90 min with an anti-rat IgG antibody combined with horseradish peroxidase (1:3000 dilution; Bio-Rad, CA, USA). The membrane was thoroughly washed and the immunocomplexes were detected using an enhanced horseradish peroxidase/luminol chemiluminescence system (ECL Plus, Amersham International plc, Little Chalfont, U.K.) and then subjected to autoradiography. Protein plots were quantified by Scion Image software (Scion based on NIH image) in arbitrary units of optical density normalized by average values measured for C samples in each membrane.

Statistical analysis

Results are expressed as means ± SEM and analyzed by Student *t*-test or by analysis of variance (one- or two-way ANOVA) followed by *post hoc* Bonferroni test, as appropriate. All statistical analyses were carried out with GraphPad Prism 4.0 (GraphPad Softwares Inc., San Diego, CA, USA) and differences of *p* < 0.05 were considered significant.

Results

Biometrics and Doppler echocardiography

Table 1 shows that right and left ventricular weights increased in the LMI group compared to controls (C group). MMI was just partially altered compared to C, with only heart/body weight

Table 1 - Cardiac parameters

	Control (n = 17)	Moderate MI (n = 10)	Large MI (n = 14)
Biometrics			
H/BW (mg g ⁻¹)	2.72 ± 0.06	3.17 ± 0.08 *	3.43 ± 0.11 *
RV/BW (mg g ⁻¹)	0.68 ± 0.02	0.74 ± 0.02	0.94 ± 0.07 *
LV/BW (mg g ⁻¹)	2.20 ± 0.05	2.52 ± 0.08 *	2.61 ± 0.07 *
PWC (%)	79 ± 0.21	80 ± 0.31	82 ± 0.48 *
Echocardiography			
LvD (cm)	0.72 ± 0.01	0.81 ± 0.02	0.98 ± 0.02 *
FS (%)	54.8 ± 2.04	37.4 ± 1.44 *	26.3 ± 1.94 **
E/A ratio	2.15 ± 0.1	2.4 ± 0.2 *	4.86 ± 0.5 * #
Infarct size (%)	–	32.8 ± 1.6	44.8 ± 1.2 #

Results are expressed as mean ± SEM. MI - Myocardial infarction; H/BW - Body weight-indexed heart; RV/BW - Ratios of right and left ventricular (LV/BW) weights to body weights; PWC - Pulmonary water content; LvD - Diastolic diameter; FS - Fractional shortening; E/A - E/A wave velocities ratio. **p* < 0.05 vs. Control and #*p* < 0.05 vs. Moderate MI. One-way ANOVA plus *post hoc* Bonferroni TEST.

and LV/body weight indexes increased. These parameters were accompanied by greater PWC in LMI than in MMI and C (Table 1). Echocardiographic morphological and functional data (Table 1) suggest existing chamber dilatation associated with systolic and diastolic dysfunction in rats from both the infarcted groups, and most of the evaluated parameters were more extensively altered in the LMI group than MMI.

Myocardial contractility in vitro

The cross sectional area was larger in LMI (1.16 ± 0.05 mm², n = 14) compared to MMI (1.01 ± 0.05 mm², n = 10) and C (0.96 ± 0.04 mm², n = 17). As seen in Table 2, after six weeks of coronary occlusion, the contractile parameters were impaired in the MMI and LMI groups compared to C, exhibiting a depression of DT and positive dT/dt. Nevertheless, only the LMI group showed significant depression of the negative dT/dt, as well as an increased time duration of contraction and relaxation phases.

In Figure 1A, original tracings illustrate the PRC behavior of papillary muscles from control and infarcted rats during pauses of stimulation. In the C group, potentiation of PRC occurred, which increased with the duration of the pause. However, in the muscles from infarcted groups, the PRC behavior was substantially changed. While MMI presented a reduction on this PRC potentiation, LMI muscles developed a decay of force after rest compared to steady state contractions. The decay was accentuated with the increase of pause duration (Figure 1B).

In order to investigate the mechanisms of PRC in papillary muscles from infarcted rats, pharmacological (Figure 2) and molecular (Figure 3) tools were used. Since only the LMI group exhibited the unusual behavior of PRC, the following pharmacological protocols were performed only in C and LMI papillary preparations. Administration of Ry (1 µM, for 30 min) in the Krebs-Henseleit solution completely abolished the PRC potentiation in C and the PRC decay in LMI (Figure 2A). On the other hand, NCX blockade with a modified Krebs-Henseleit solution containing Li⁺ instead of Na⁺ promoted a slight enhancement of the relative PRC contraction in C and reestablished normal behavior in LMI, converting the PRC decay to a PRC potentiation profile (Figure 2B).

Table 2 - Papillary muscle mechanics in Lmax

	Control (n = 17)	Moderate MI (n = 10)	Large MI (n = 14)
DT (g mm ⁻²)	5.04 ± 0.41	4.03 ± 0.18 *	2.9 ± 0.20 * #
RT (g mm ⁻²)	1.15 ± 0.07	1.19 ± 0.12	1.48 ± 0.16 *
+dT/dt _{max} (g mm ⁻² s ⁻¹)	53.35 ± 4.43	40.26 ± 1.93 *	25.76 ± 2.33 * #
-dT/dt _{max} (g mm ⁻² s ⁻¹)	-31.04 ± 2.44	-22.57 ± 1.00	-19.60 ± 1.93 *
TPT (ms)	157 ± 8	175 ± 8	210 ± 6 *
TR50 (ms)	149 ± 10	162 ± 9	202 ± 7 *

Results are expressed as mean ± SEM of developed tension (DT); MI - Myocardial infarction; RT - Resting tension; +dT/dt_{max} - maximum rate of tension development and decline (-dT/dt_{max}); TPT - Time to peak tension; TR50 - Time to 50% relaxation. **p* < 0.05 vs. Control and #*p* < 0.05 vs. Moderate MI. One-way ANOVA plus *post hoc* Bonferroni test.

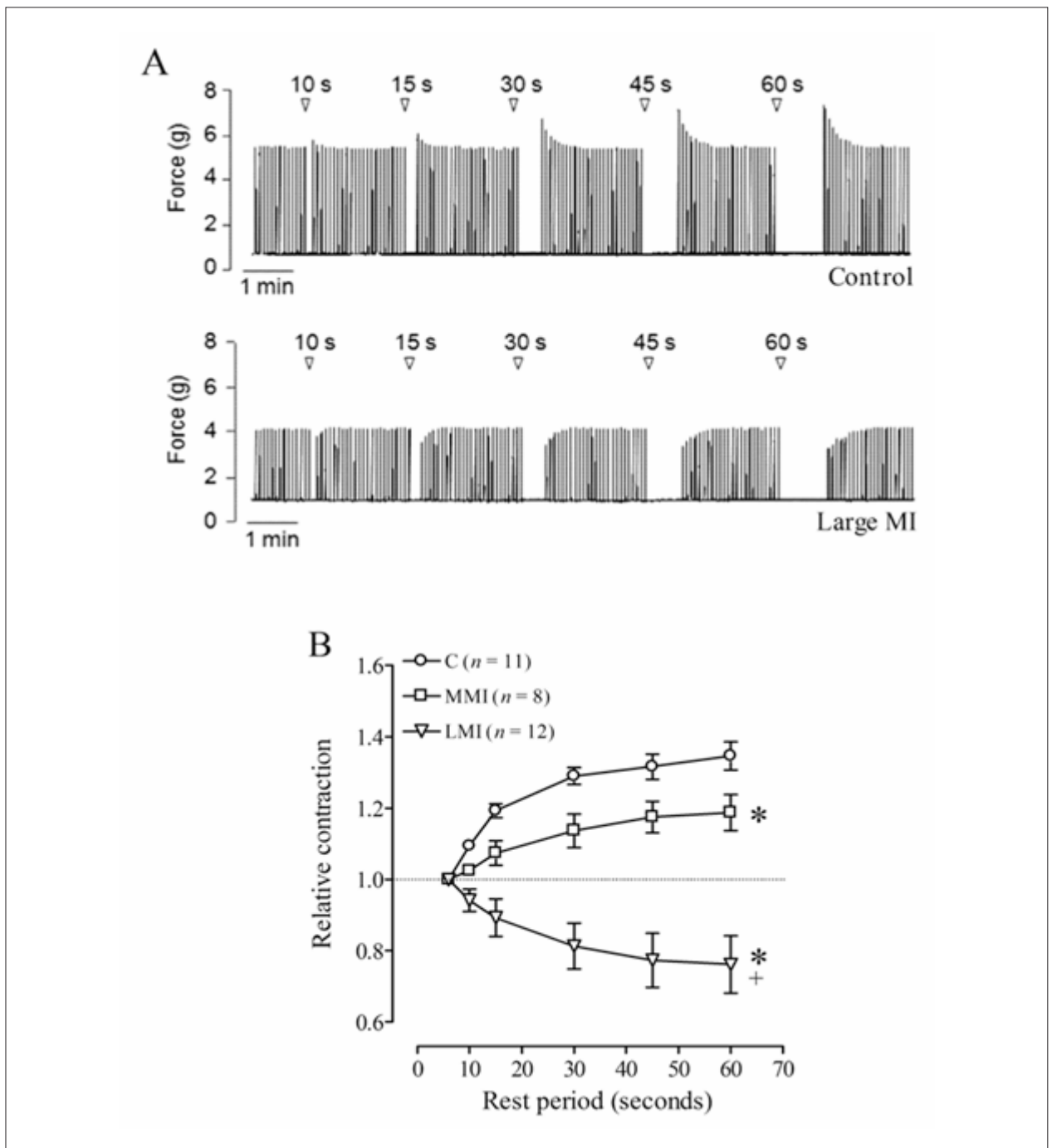


Figure 1 - Post-rest contraction of isolated papillary muscle preparations. Panel A, typical tracings representing developed force of the papillary muscle from control (upper) and large MI (lower) rats before and after pauses of stimulation (10 to 60 sec). Potentiation of post-rest contractions is evidenced in control while post-rest decays of force occurred in the muscle from large MI rats. Panel B, Effect of increasing (mean \pm SEM) pause durations on the relative contraction (PRC divided by steady state contraction) of control (C), moderate (MMI) and large infarct (LMI) groups. Two-way ANOVA plus post hoc Bonferroni tests for data * $p < 0.05$ vs. C. * $p < 0.05$ vs. MMI.

Protein content by Western blotting

Calcium handling proteins potentially involved in these alterations were investigated in all groups (Figure 3). The myocardial remodeling after infarction led to a decrease in SERCA2 content; although MMI moderately decreased SERCA2 protein expression,

significance was reached only for the LMI group (Figure 3A). Total PLB was significantly reduced in both MMI ($79 \pm 12\%$ of C content) and LMI ($65 \pm 10\%$ of C content); its phosphorylated form (Ser¹⁶-PLB) was also reduced in the infarcted groups (Figure 3B). Although NCX protein content did not change in MMI when compared to C, it was approximately 1.7-fold overexpressed in LMI (Figure 3C).

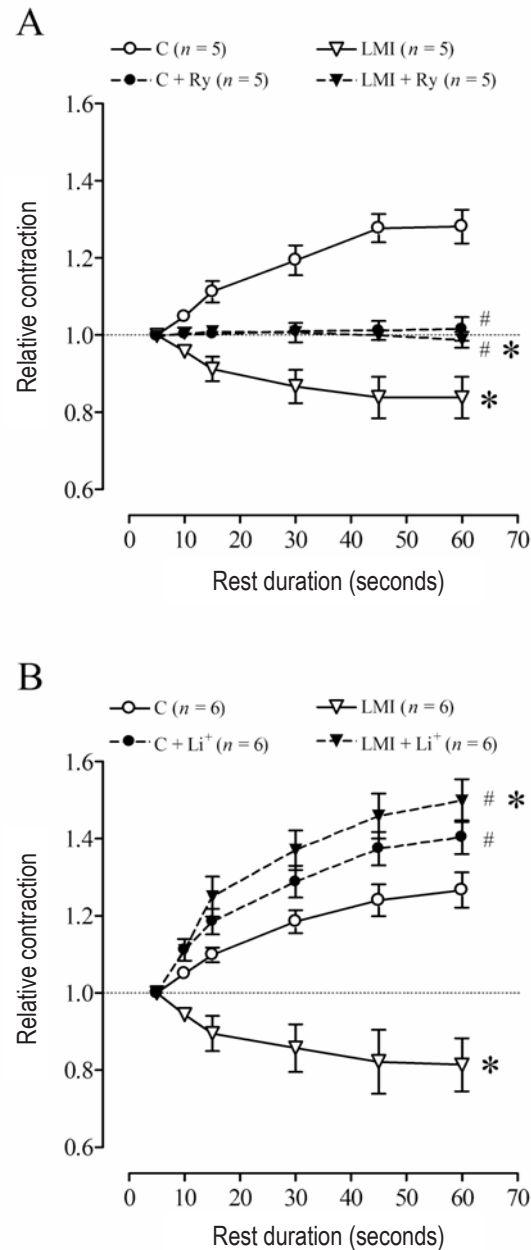


Figure 2 - Effects of ryanodine (Ry) and lithium chloride (Li⁺) on post-rest contractions. Panel A, Post-rest potentiation and decay of contractions were abolished after the addition of 1 μ M Ry in preparations of control (C) and large infarct (LMI) groups, respectively. Panel B, substitution of Li⁺ for sodium in the buffer solution enhanced post-rest potentiation in C and conversion of decay to potentiation in LMI. * $p < 0.05$ vs. C group without pharmacological interventions. # $p < 0.05$ vs. before Ry or Li⁺. Two-way ANOVA plus post hoc Bonferroni test. Symbols represent mean \pm SEM.

Discussion

In this study, we demonstrated that myocardial remodeling after MI in rats may change the regular post-rest potentiation to post-rest decay of active force by affecting myocyte Ca²⁺ handling proteins. This uncommon behavior of myocardial mechanics was evident only in animals with large infarcts, in which the remodeling process included not only LV dilation with systolic and

diastolic dysfunction, but also worse myocardial contraction and relaxation probably due to impaired SR Ca²⁺ uptake and excessive sarcolemmal Ca²⁺ efflux.

MI ventricular dysfunction and chamber dilatation, normally observed in rats with larger infarctions²³, are also shown in this study. Post-MI remodeling was associated with a depressed tension development in papillary muscles from infarcted rats and reduced

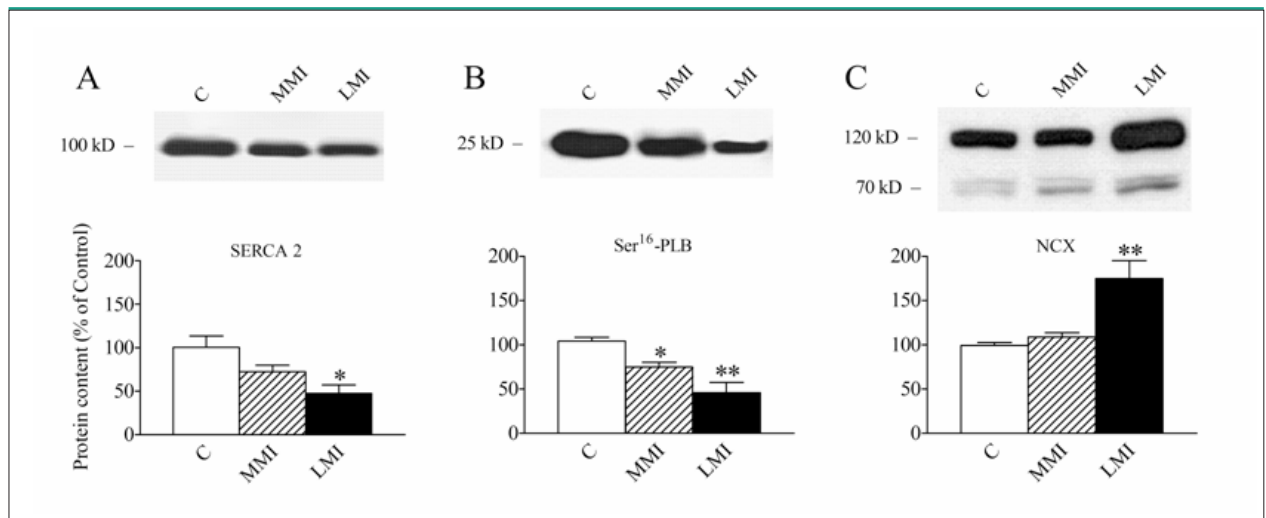


Figure 3 - Protein content of SERCA2, Ser¹⁶-PLB and NCX by western blotting. Protein contents of SERCA2 (Panel A) and Ser¹⁶-PLB (Panel B) were decreased in moderate (MMI, $n = 4$) and large infarct (LMI, $n = 4$) groups when compared to control (C, $n = 5$); NCX (Panel C) was overexpressed only in LMI myocardium. Data (mean \pm SEM) are expressed as the percentage of the control group. * $p < 0.05$; ** $p < 0.01$ vs. C; and $+p < 0.05$ vs. MMI. One-way ANOVA plus post hoc Bonferroni test.

rate of force generation and relaxation, as previously reported for papillary muscles^{9,10,13,20,24}. Similar impairment of shortening was identified in isolated ventricular myocytes as well^{25,26}, and the proposed mechanisms explaining the contractile dysfunction include defects in the excitation-contraction coupling^{13,24}.

Post-rest contractions in cardiac muscle

During myocardial rest, Ca²⁺ is removed from the cytosol into the SR by SERCA2 or into the mitochondria by the Ca²⁺-uniporter, or it is extruded by the sarcolemmal NCX and Ca²⁺-ATPase¹. In the PRC protocols such as that used in this work, a potentiation of DT occurs after a pause of stimuli as expected for the rat cardiac muscle. Normally, as most of the Ca²⁺ returns to the SR during the rest period, its content tends to increase with increased duration of the pause, also increasing Ca²⁺ release and, finally, the force generation upon the next activation¹. In fact, the administration of Ry to block SR function in our experiments completely abolished the PRC potentiation of C muscles, reinforcing previous reports describing the key role of SR storing function in this phenomenon⁴. On the other hand, the inhibition of transsarcolemmal Ca²⁺ extrusion by NCX in our preparations (by using Li⁺) enhanced the potentiation of C muscles, which confirms the importance of Ca²⁺ efflux mechanisms to negatively modulate the PRC of rat LV muscle^{6,7}. Indeed, it was reported that the stimulation of NCX leads to an increasing Ca²⁺ efflux and Na⁺ influx, and consequently, a depression of the PRC^{27,28}.

Post-rest decay in rat cardiac muscle

Several reports investigated the myocardial remodeling post-infarct contractile dysfunction and pointed out impairments on the cardiomyocyte Ca²⁺ movement^{13,29-31}. The literature is controversial concerning the behavior of PRC in post-MI remodeling. In human failing myocardium, authors reported either depressed potentiation^{32,33} or decay²⁸ of contraction after prolonged pauses. In animal models^{9,10},

depressed potentiation compared to controls were reported from infarcted rats. Also, in surviving myocytes after MI in dogs, there was a diminished potentiation of contraction after rest³⁴. These alterations have been attributed essentially to the defective SR storing function, associated with a relative reduction of released Ca²⁺. Recently, our group identified decay of PRC on the papillary muscles from heart failure rats 40 weeks after coronary occlusion¹⁶. However, the causal mechanisms for this unprecedented PRC behavior in rats were not investigated, as in this study used adult rats with healed six-week-old infarcts.

Our experiments suggest that excitation-contraction coupling alterations contribute to the depression of PRC in LMI rats: the SR storing dysfunction was associated with enhanced Ca²⁺ extrusion, since Ry abolished this phenomenon while NCX inhibition normalized it.

The impaired SR reuptake function, which probably occurs in both MMI and LMI groups, may not be due only to the decreased protein expression of SERCA2, but also to the lower Ser¹⁶-PLB content as evidenced by the Western blotting assays. When phosphorylated, the regulatory protein PLB relieves the inhibition of SERCA2, allowing its Ca²⁺ uptake function¹. In fact, the decreased PLB phosphorylation in remodeled myocardium of infarcted rats has also been described as leading to SR dysfunction³¹. Moreover, we cannot exclude that a high diastolic Ca²⁺ leak from SR vesicles is occurring. It has been reported that Ry receptor regulatory proteins (FKBP, especially FKBP12.6) can be pathologically altered in structure and content, as well as in phosphorylation mechanisms that modulate the FKBP-ryanodine receptor coupling, resulting in a sub-conductance status in myocardium remodeling^{29,35}. Especially in LMI muscles, using Li⁺ instead of Na⁺ in the Krebs-Henseleit solution, the PRC decay in LMI experiments changed to a typical PRC potentiation, suggesting the key role of NCX on the weakness of subsequent contraction when PRC decay occurs. As mentioned before, although Ca²⁺

SR accumulation is relatively limited by the Ca^{2+} efflux through the sarcolemma, SR normally re-uptakes most of Ca^{2+} as a result of the dominant SERCA2 uptake over the transsarcolemmal extrusion of this ion in rat cardiomyocyte. On the other hand, while sarcolemmal Ca^{2+} efflux mechanisms are playing a more important role than that of the SR re-uptake, a decay of SR Ca^{2+} content tends to occur with a longer duration of pause in rabbits²⁷. Actually, in mammals in which the importance of SERCA2 is counteracted by NCX in carrying out the Ca^{2+} withdrawal, such as the rabbits, the myocardium normally exhibits this reduction in the force of the first contraction following the rest proportionally to the pause duration, referred to as post-rest decay¹. In fact, our results show a significant overexpression of NCX content in LMI compared to the MMI and C groups, thus supporting the idea that increased NCX activity and/or expression relates to post-rest decay after MI and heart failure, at least in rats.

Although the remodeled myocardium from both MMI and LMI groups decreased SERCA2 and Ser¹⁶-PLB contents, an increase of the NCX protein level was observed only in LMI, the experimental group that exhibited post-rest decay. Thus, the molecular profile with post-MI remodeling should be a critical variable for post-rest decay occurrence. Actually, changes in different cardiomyocyte proteins were reported in animal models^{21,30,36} and humans with heart failure^{37,38} as causing dysfunctional excitation-contraction coupling. As a result, we suggest that the altered importance of transsarcolemmal Ca^{2+} efflux caused by overexpressed NCX associated with dysfunctional SR uptake probably led the rat failing myocardium to exhibit this PRC decay.

Although we have not measured directly the $[\text{Ca}^{2+}]_i$ or the activity of calcium-handling proteins analyzed, we recognize

limitations in this study. Our results suggest that impaired SR reuptake function associated with an increased calcium efflux during diastole of muscle from LMI is the probable cause of the post-rest decay of force. Therefore, it is also possible to speculate that although lower $[\text{Ca}^{2+}]_i$ due to increased NCX reduces the deleterious Ca^{2+} overload, it may reduce the Ca^{2+} available for reuptake during diastole and consequently the amount released during systole.

In summary, our results confirmed that infarcted rats present global ventricular dysfunction and contractile myocardial disturbances derived from infarction directly related to the severity of the remodeling. Contributing to that alteration, the use of PRC protocol identified an exceptional behavior of rat myocardium, assigned as post-rest decay of force. This phenomenon is ascribed to a disorder of Ca^{2+} handling proteins in carrying out normal functions, particularly in large myocardial infarctions, due to the association of reduced Ca^{2+} re-uptake by SERCA2 with excessive Ca^{2+} efflux by NCX.

Potential Conflict of Interest:

No potential conflict of interest relevant to this article was reported.

Sources of Funding:

There were no external funding sources for this study.

Study Association:

This study is not associated with any post-graduation program.

References

1. Bassani JWM, Bassani RA, Bers DM. Relaxation in rabbit and rat cardiac cells: species-dependent differences in cellular mechanisms. *J Physiol*. 1994;476(2):279-93.
2. Bers DM. Calcium cycling and signaling in cardiac myocytes. *Annu Rev Physiol*. 2008;70:23-49.
3. Endoh M. Force-frequency relationship in intact mammalian ventricular myocardium: physiological and pathophysiological relevance. *Eur J Pharmacol*. 2004;500(1-3):73-86.
4. Ravens U, Link S, Gath J, Noble M. Post-rest potentiation and its decay after inotropic interventions in isolated rat heart muscle. *Pharmacol Toxicol*. 1995;76(1):9-16.
5. Rossoni LV, Xavier FE, Moreira CM, Falcochio D, Amanso AM, Tanoue CU, et al. Ouabain-induced hypertension enhances left ventricular contractility in rats. *Life Sci*. 2006;79(16):1537-45.
6. Abreu G, Vassallo D, Mill J. The $\text{Na}^+/\text{Ca}^{2+}$ exchange mechanism as a regulator of post rest contractions in cardiac muscle. *Braz J Med Biol Res*. 1987;20(6):817-20.
7. Mill J, Vassallo D, Leite C. Mechanisms underlying the genesis of post-rest contractions in cardiac muscle. *Braz J Med Biol Res*. 1992;25(4):399-408.
8. Stefanon I, Martins M, Vassallo D, Mill J. Analysis of right and left ventricular performance of the rat heart with chronic myocardial infarction. *Braz J Med Biol Res*. 1994;27(11):2667-79.
9. Novaes M, Stefanon I, Mill J, Vassallo D. Contractility changes of the right ventricular muscle after chronic myocardial infarction. *Braz J Med Biol Res*. 1996;29(12):1683-90.
10. Wagner KD, Theres H, Born A, Strube S, Wunderlich N, Pfitzer G, et al. Contractile function of papillary muscle from rats with different infarct size after beta-adrenergic blockade and ACE-inhibition. *J Mol Cell Cardiol*. 1997;29(11):2941-51.
11. Portes LA, Tucci PJF. Swim training attenuates myocardial remodeling and the pulmonary congestion in wistar rats with secondary heart failure to myocardial infarction. *Arq Bras Cardiol*. 2006;87(1):54-9.
12. Gomez AM, Guatimosim S, Dilly KW, Vassort G, Lederer WJ. Heart failure after myocardial infarction: altered excitation-contraction coupling. *Circulation*. 2001;104(6):688-93.
13. Sjaastad I, Birkeland J, Ferrier G, Howlett S, Skomedal T, Bjørnerheim R, et al. Defective excitation-contraction coupling in hearts of rats with congestive heart failure. *Acta Physiol Scand*. 2005;184(1):45-58.
14. O'Rourke B, Kass DA, Tomaselli GF, Kaab S, Tunin R, Marban E. Mechanisms of altered excitation-contraction coupling in canine tachycardia-induced heart failure, I: experimental studies. *Circ Res*. 1999;84(5):562-70.
15. Pogwizd SM, Qi M, Yuan W, Samarel AM, Bers DM. Upregulation of $\text{Na}^+/\text{Ca}^{2+}$ exchanger expression and function in an arrhythmogenic rabbit model of heart failure. *Circ Res*. 1999;85(11):1009-19.

16. Helber J, dos Santos AA, Antonio EL, Flumignan RLG, Bocalini, DS, Piccolo C, et al. Digoxin prolongs survival of female rats with heart failure due to large myocardial infarction. *J Card Fail.* 2009;15(9):798-804.
17. dos Santos L, Antonio EL, Souza AFM, Tucci PJF. Use of afterload hemodynamic stress as a practical method for assessing cardiac performance in rats with heart failure. *Can J Physiol Pharmacol.* 2010;88(7):724-32.
18. dos Santos L, Mello AF, Antonio EL, Tucci PJ. Determination of myocardial infarction size in rats by echocardiography and tetrazolium staining: correlation, agreements, and simplifications. *Braz J Med Biol Res.* 2008;41(3):199-201.
19. Bocalini DS, Veiga ECA, Souza AFM, Levy RF, Tucci PJF. Exercise training-induced enhancement in myocardial mechanics is lost after two-weeks of detraining in rats. *Eur J Appl Physiol.* 2010;109(5):909-14.
20. Mill J, Novaes M, Galon M, Nogueira J, Vassallo D. Comparison of the contractile performance of the hypertrophied myocardium from spontaneous hypertensive rats and normotensive infarcted rats. *Can J Physiol Pharmacol.* 1998;76(4):387-94.
21. Smith GL, Allen DG. Effects of metabolic blockade on intracellular calcium concentration in isolated ferret ventricular muscle. *Circ Res.* 1988;62(6):1223-36.
22. Romero-Calvo I, Ocón B, Martínez-Moya P, Suárez MD, Zarzuelo A, Martínez-Augustin O, et al. Reversible Ponceau staining as a loading control alternative to actin in Western blots. *Anal Biochem.* 2010;401(2):318-20.
23. Litwin SE, Katz SE, Morgan JP, Douglas PS. Serial echocardiographic assessment of left ventricular geometry and function after large myocardial infarction in the rat. *Circulation.* 1994;89(1):345-54.
24. Litwin SE, Litwin CM, Raya T, Warner A, Goldman S. Contractility and stiffness of noninfarcted myocardium after coronary ligation in rats: effects of chronic angiotensin converting enzyme inhibition. *Circulation.* 1991;83(3):1028-37.
25. Wisløff U, Loennechen JP, Currie S, Smith GL, Ellingsen O. Aerobic exercise reduces cardiomyocyte hypertrophy and increases contractility, Ca²⁺ sensitivity and SERCA-2 in rat after myocardial infarction. *Cardiovasc Res.* 2002;54(1):162-74.
26. Zhang X-Q, Song J, Qureshi A, Rothblum LI, Carl LL, Tian Q, et al. Rescue of contractile abnormalities by Na⁺/Ca²⁺ exchanger overexpression in postinfarction rat myocytes. *J Appl Physiol.* 2002;93(6):1925-31.
27. Bassani RA, Bers DM. Na-Ca exchange is required for rest-decay but not for rest-potential of twitches in rabbit and rat ventricular myocytes. *J Mol Cell Cardiol.* 1994;26(10):1335-47.
28. Maier LS, Schwan C, Schillinger W, Minami K, Schutt U, Pieske B, Geringerol, isoproterenol and ouabain normalize impaired post-rest behavior but not force-frequency relation in failing human myocardium. *Cardiovasc Res.* 2000;45(4):913-24.
29. Marx SO, Reiken S, Hisamatsu Y, Jayaraman T, Burkhoff D, Rosembly N, et al. PKA phosphorylation dissociates FKBP12.6 from the calcium release channel (ryanodine receptor): defective regulation in failing hearts. *Cell.* 2000;101(4):365-76.
30. Gomez AM, Schwaller B, Porzig H, Vassort G, Niggli E, Egger M. Increased exchange current but normal Ca²⁺ transport via Na⁺-Ca²⁺ exchange during cardiac hypertrophy after myocardial infarction. *Circ Res.* 2002;91(4):323-30.
31. Bers DM. Altered cardiac myocyte Ca regulation in heart failure. *Physiology.* 2006;21:380-7.
32. Pieske B, Maier LS, Bers DM, Hasenfuss G. Ca²⁺ handling and sarcoplasmic reticulum Ca²⁺ content in isolated failing and nonfailing human myocardium. *Circ Res.* 1999;85(1):38-46.
33. Rossman EI, Petre RE, Chaudhary KW, Piacentino V, Janssen PML, Gaughan JP, et al. Abnormal frequency-dependent responses represent the pathophysiologic signature of contractile failure in human myocardium. *J Mol Cell Cardiol.* 2004;36(1):33-42.
34. Licata A, Aggarwal R, Robinson RB, Boyden P. Frequency dependent effects on Ca_i transients and cell shortening in myocytes that survive in the infarcted heart. *Cardiovasc Res.* 1997;33(2):341-50.
35. Yano M, Yamamoto T, Ikemoto N, Matsuzaki M. Abnormal ryanodine receptor function in heart failure. *Pharmacol Ther.* 2005;107(3):377-91.
36. Wasserstrom JA, Holt E, Sjaastad I, Lunde PK, Odegaard A, Sejersted OM. Altered E-C coupling in rat ventricular myocytes from failing hearts 6 wk after MI. *Am J Physiol Heart Circ Physiol.* 2000;279(2):H798-807.
37. Hasenfuss G, Reinecke H, Studer R, Pieske B, Meyer M, Drexler H, et al. Calcium cycling proteins and force-frequency relationship in heart failure. *Basic Res Cardiol.* 1996;91(Suppl.2):17-22.
38. Prestle J, Quinn FR, Smith GL. Ca²⁺-handling proteins and heart failure: novel molecular targets? *Curr Med Chem.* 2003;10(11):967-81.

